EARLY DETECTION OF PARKINSON'S DISEASE THROUGH SHAPE BASED FEATURES FROM ^{123}I-IOFLUPANE SPECT IMAGING

Noopur A. Bhalchandra[1], R. Prashanth[1], Sumantra Dutta Roy[1], Santosh Noranha[2]

[1]Department of Electrical Engineering, Indian Institute of Technology Delhi, New Delhi, India
[2]Department of Chemical Engineering, Indian Institute of Technology Bombay, Mumbai, India

ABSTRACT

Detection of Parkinson's disease (PD) at an early stage is important for effective management and for initiating neuroprotective strategies early in the therapeutic process. Single photon emission computed tomography (SPECT) using ^{123}I-Ioflupane (DaTSCAN^{TM}, GE Healthcare; also known as [123I]FP-CIT) have shown to be a sensitive marker for PD even in the early stages of the disease. In this paper, we carry out image processing to compute shape-based features which are radial and gradient features from SPECT scans from 163 early-stage PD and 187 healthy normal subjects obtained from the Parkinson's Progression Markers Initiative (PPMI), and use them along with the striatal binding ratio (SBR) values, also provided by the PPMI as features to classify between the two using Discriminant Analysis and Support Vector Machine (SVM). We observe a high accuracy of 99.42% in classification. It is inferred that such models can aid clinicians in the early diagnostics of PD.

Index Terms— Parkinson's disease, Computer-aided early detection, Pattern analysis, Linear Discriminant Analysis (LDA), Support Vector Machine (SVM)

1. INTRODUCTION

Parkinson's disease (PD) is the second most common neurodegenerative disorder significantly affecting the quality of lives of the affected people [1]. It is a progressive disorder which is characterized by a number of motor as well as non-motor symptoms. As of now, all the therapeutic options focus on symptomatic relief [2, 3]. Non-availability of any definitive tests make clinical criteria the sole basis for diagnosing PD. Cardinal Symptoms such as bradykinesia, rigidity and tremor at rest are characterized clinically [2]. The clinical diagnosis often happens with onset of these symptoms in the advanced stages correlated with decline in 60-80% dopamine (DA) concentrations and 40–50% degeneration of cell bodies in the substantia nigra pars compacta (SNc) [3].

A non-linear course of progression is followed in PD and the deterioration is rapid during the early stages, making early detection important [2]. Early and accurate detection of PD is also crucial for effective management. The PPMI, a landmark and large-scale study, is an effort in this direction. It primarily focuses on identifying PD progression markers that can aid in early detection of the disease [4].

Single Photon Emission Computed Tomography (SPECT) is becoming a popular imaging technique that can be used for inspecting the dopaminergic systems in the human brain *in vivo*. [123I]FP-CIT SPECT has shown to be sensitive in differentiating PD from healthy normal subjects by depicting the dopaminergic transporter (DAT) loss, even in the subclinical stages of PD [5]. Due to this loss, there is a change of shape in the appearance of the striatal dopaminergic activity in the SPECT scans.

Clinically, SPECT scans are usually visually assessed. The striatal binding ratio (SBR) value is a quantified parameter that is obtained after performing region-based analysis on SPECT images. It quantifies the striatal activity and is also used clinically when in doubt or for borderline cases [6]. The use of image analysis for feature extraction and pattern recognition techniques is new and is becoming popular in the area of PD detection [7-11]. Prashanth *et al*. in [7] carried out analysis on SPECT images of 20 healthy normal, 20 early-stage PD and 20 scans without evidence of dopaminergic deficit (SWEDD-they are subjects who are clinically diagnosed as PD but show normal SPECT scans) to extract shape-based features corresponding to the high activity regions of the striatum. However, it did not include any classification. There also have been studies carrying out voxel-based analysis on the SPECT data. Towey *et al*. [8] carried out Singular Value Decomposition (SVD) for extracting the significant voxels, and then used Naïve Bayes (NB) for the classification of Parkinsonian Syndrome (PS) or non-PS. [9-11] distinguished normal controls from PS based on information from the voxels of striatum. [9] used principal component analysis (PCA) followed by SVM for classification. [10, 11] also used SVM classifier for classification. However, [12] suggest that voxel-based technique is not recommended and validated in routine clinical setting as it involves warping of images to a template image followed by smoothing of image data sets.

In this work, we carry out image analysis to segment the high activity regions (which correspond to the concentration of striatal dopamine transporter) and compute shape-based radial and gradient features. We use these features along with the SBR values obtained from the PPMI to carry out classification of early-stage PD from healthy normal.

2. MATERIALS AND METHODS

The flowchart of the analysis carried out in the study is shown in Fig. 1.

2.1. Database

Data used in the preparation of this article were obtained from the PPMI database (www.ppmi-info.org/data). For up-to-date information on the study, please visit www.ppmi-info.org. The PPMI is a large-scale, comprehensive, observational, international,

multi-center study designed to identify PD progression biomarkers. We have used SPECT images of 163 early-stage PD (Hoehn and Yahr stage I or II) and 187 healthy normal subjects from the database.

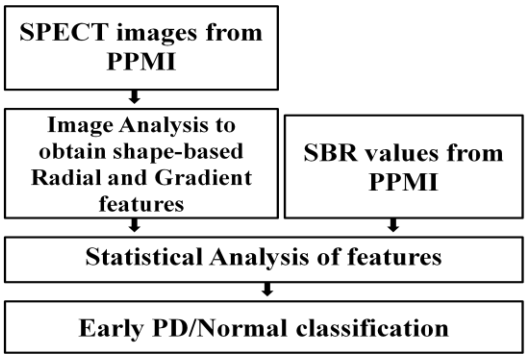

Fig. 1. Flowchart of the analysis carried out.

2.2. Image analysis and feature extraction

2.2.1. Preprocessing by PPMI

The SPECT scans acquired at the PPMI sites undergo initial preprocessing of reconstruction from raw projection data along with attenuation correction using phantoms obtained from the same day subject is imaged. They also carry out spatial normalization of the images for consistency in orientation [13]. Each scan provided by the PPMI database consists of a set of 91 axial slices (from top to bottom of the head). We select the 42nd slice which we have intensity normalized for further analysis as this slice clearly showed the striatal activity.

2.2.2. Segmentation and boundary detection

We carry out analysis of the high activity regions by segmenting it followed by quantification using shape-based features. The segmentation was carried out by converting the image to a binary using threshold in the range [0.8-0.9]. The threshold is empirically chosen based on observing the segmentation of the high activity regions. Followed by segmentation, boundaries of these regions were detected using Canny edge detection method. The boundaries of the striatum were visually assessed by an expert neurologist and a radiologist. Fig. 2 shows the SPECT slices from a healthy normal and early-stage PD subject, along with the detected boundary of the segmented regions.

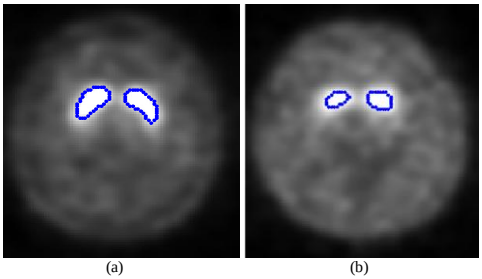

(a) (b)

Fig. 2. (a) Control SPECT slice and (b) Early PD SPECT slice with blue boundary of the segmented regions.

2.2.3. Feature description

Discrimination of the PD from normal is carried out based on following three features.

SBR values: PPMI SPECT imaging lab extracts regional count densities in regions with the help of a standardized volume of interest template. Striatal Binding Ratio (SBR) values are count densities of each of the 4 striatal regions: left, right caudate and left, right putamen calculated with reference to occipital cortex. Detailed approach followed by PPMI in calculation of SBR is provided on [14]

$$SBR = \frac{Target\ region\ count\ density}{Reference\ region\ count\ density} - 1$$

where, Target region: left caudate, right caudate, left putamen, right putamen. Reference region: occipital cortex.

First feature vector thus formed consists: average of left, right putamen as one value and average of left, right caudate as second.

Radial feature: The second set of feature is radial feature vector [15]. The boundary pixels of each striatum are sampled at an equal angular interval of 45° (assumed 0° along horizontal axis and angles measured in clockwise direction) giving 8 sampled points from 0° through 360° for each striatum. This sampling for the right striatum is done on its vertically flipped version so that all calculations are with reference to left striatum. The radial distances of these sampled points from the respective centroids of the striata are computed as can be seen in fig. 3(a). An average radius of each of the sampled points of left striatum with its corresponding same numbered sampled points in right striatum forms the feature vector (1-by-8 dimensional).

Table 1. Radial feature set corresponding to angles.

0°	45°	90°	135°	180°	225°	270°	360°
Rad 1	Rad 2	Rad 3	Rad 4	Rad 5	Rad 6	Rad 7	Rad 8

Gradient feature: The third feature set involves determination of gradients [16]. The eight sampled points as above, when joined through a line segment, form a polygon along the boundary. These are considered for each of the striatum as in Fig. 3(b). Gradients of the segments for respective striatum are calculated where right striatum is again vertically flipped prior to all computations. Gradient feature vector is the average of the gradients of same numbered segments as depicted in Fig, 3(b) of both the striata having dimensionality 1-by-8.

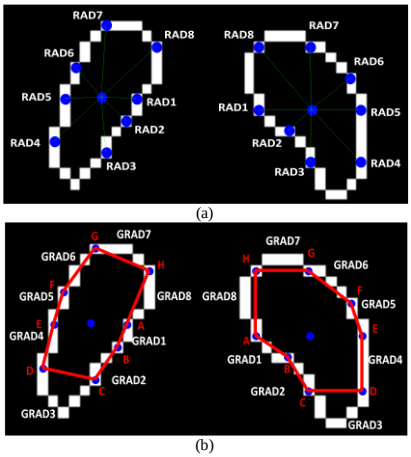

Fig. 3. (a) Rad1 to Rad8 are the radii of 8 sampled points with respect to the centroid. (b) Grad1 to Grad8 are gradients of the segments joining sampled points.

2.3. Statistical testing of features

The final feature set (1 by 18 dimension) which is further tested for statistical significance is formed by concatenating 2 SBR values, 8 radial values and 8 gradient values. Features being 'non'-normally distributed, Wilcoxon rank sum test is carried out to obtain the *p*-values and *z* score, where *p*-value is the significance of the regression coefficient and *z* scores are standard deviations. The threshold of significance is defined as a value of $p < 0.05$.

Table 2. Result of statistical testing of each feature.

Features	*p* value	*z* score	Features	*p* value	*z* score
SBRcaud	.000	-14.508	Rad8	.000	-16.103
SBRputa	.000	-15.980	Grad1	.000	-7.361
Rad1	.000	-8.733	Grad2	.000	15.271
Rad2	0.398	-0.846	Grad3	.000	4.073
Rad3	.000	-15.489	Grad4	.000	-15.541
Rad4	.000	-15.992	Grad5	0.434	0.782
Rad5	.000	-13.359	Grad6	0.159	1.407
Rad6	.000	-14.859	Grad7	0.002	3.148
Rad7	.000	-16.069	Grad8	.000	-15.08

2.4. Classification of early PD/ Normal

Classification is done with two classifiers for comparing their performances: Linear Discriminant Analysis (LDA) and Binary Support Vector Machine (SVM) classifier with linear and RBF kernels. LDA is employed with 10 fold cross validation while 5 fold cross validation is used to train and test the SVM.

3. RESULTS AND DISCUSSION

Images which were not included in this study off the total early PD and healthy normal PPMI image collection were above H and Y stage II or very degenerated. Also 2% of them did not have either SBR values or SPECT scans.

3.1. Statistical significance

The shape change of striata in PD and control is clearly depicted in Fig. 2 (b) and (a). This shape alteration is captured significantly by the 15 feature vectors from 18. The value of these significant feature vectors for control and Early PD in the form of box plots are shown in Fig. 4. It can be noticed that there is appreciable amount of variation in both the classes for the shown features. The 3 left out feature vectors Rad2, Grad5 and Grad6 have $p>0.05$ as in Table 2 and are hence discarded.

Grad5 and Grad6 are gradients of the two segments joining the boundary points of caudate nucleus Fig. 3 (b). Changes in these two gradient values are consistently smaller for control and early PD than other gradient values making them non-discriminatory. These results are in agreement with the clinical findings suggesting degeneration in putamen is more and precede changes in caudate substantially in early stages of PD [17].

Feature vector Rad2 of sampled boundary point B is on the concave part, essentially anterior putamen of both the striatum Fig. 3(a). This radial value on an average for early PD and normal subjects is almost similar and hence statistically insignificant. According to the studies, progression of PD marks worsening of posterior putamen first with 77% reduction then anterior putamen (60% reduction) and caudate nucleus (44% reduction) [18, 19]. Reduction of posterior putamen and caudate head does not shift the centroid of the striatum much making no considerable changes in Rad2, while boundary points in posterior putamen and in caudate nucleus come closer to centroids compared to normal Striata reducing their radial distance.

3.2. Future work

The presented model can also be used for detection and classification of other classes of subjects like prodromal, Essential Tremor (ET) and SWEDD.

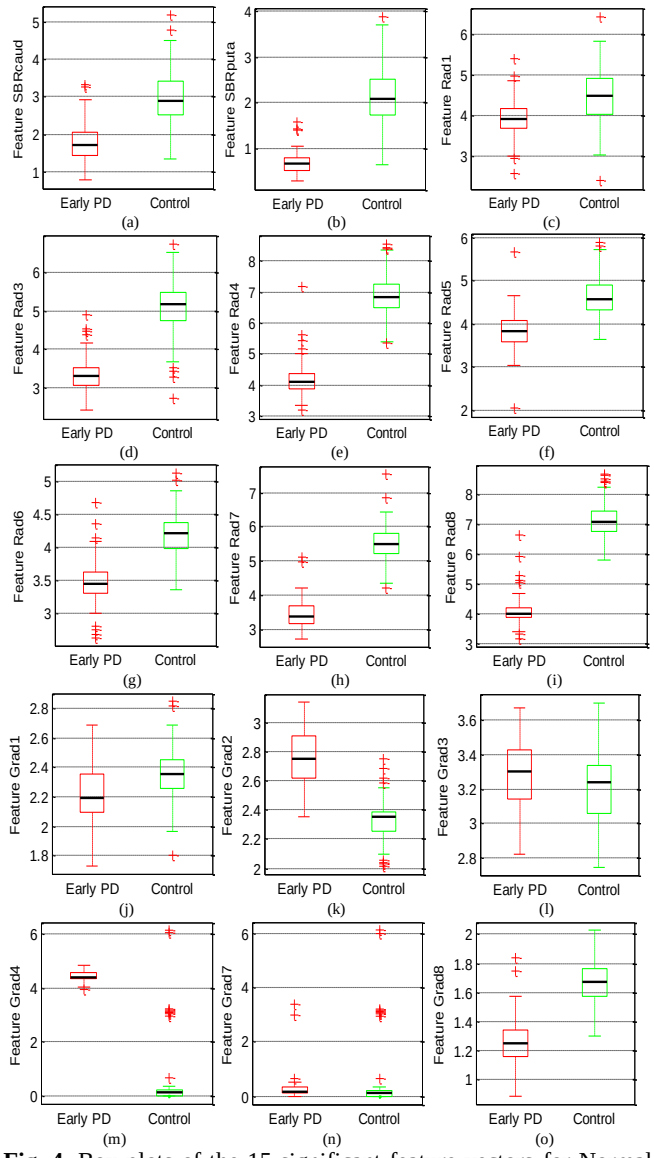

Fig. 4. Box plots of the 15 significant feature vectors for Normal and Early PD.

Table 3. Classification results with different classifiers.

Classifiers	LDA	SVM (Linear kernel)	SVM (RBF kernel)
Accuracy	99.34%	99.42%	99.42%

Classification with LDA and SVM (with both kernels) obtained 99% accuracy.

4. CONCLUSION

Early Parkinson's disease detection using machine learning is gaining importance since clinically PD can be detected in a person only at advanced stages when neuroprotective therapies may have fewer effects on progression of the PD. Hence the biomarkers presented in this work prove helpful in detection of the disease in early stages. The striatal binding ratios, radial distribution features along with gradient features give 99% accuracy and thus can aid the medical community.

ACKNOWLEDGEMENT

PPMI – a public-private partnership – is funded by the Michael J. Fox Foundation for Parkinson's Research and funding partners, including Abbvie, Avid, Biogen Idec, Bristol-Myers Squibb, Covance, GE Healthcare, Genentech, GlaxoSmithKline, Lilly, Lundbeck, Merck, Meso Scale Discovery, Pfizer Inc., Piramal, F. Hoffman-La Roche Ltd., and UCB. Authors also thank Dr. Makarand Kanjalkar (Neurologist) and Dr. Prashant Deshpande (Radiologist) for their valuable comments.

5. REFERENCES

[1] L. M. de Lau and M. Breteler, "Epidemiology of Parkinson's disease," *The Lancet Neurology*, vol. 5, pp. 525-535, 2006.

[2] J. Jankovic, "Parkinson's disease: clinical features and diagnosis," *Journal of Neurology, Neurosurgery & Psychiatry*, vol. 79, pp. 368–376, 2008.

[3] A. E. Lang and J. A. Obeso, "Challenges in Parkinson's disease: restoration of the nigrostriatal dopamine system is not enough," *The Lancet Neurology*, vol. 3, pp. 309-316, 2004.

[4] K. Marek, D. Jennings, S. Lasch, A. Siderowf, C. Tanner, T. Simuni, C. Coffey, K. Kieburtz, E. Flagg, and S. Chowdhury, "The parkinson progression marker initiative (PPMI)," *Progress in neurobiology*, vol. 95, pp. 629-635, 2011.

[5] J. Booij, G. Tissingh, G. J. Boer, J. D. Speelman, J. C. Stoof, A. G. Janssen, E. C. Wolters, and E. A. Van Royen, "[123I]FP-CIT SPECT shows a pronounced decline of striatal dopamine transporter labelling in early and advanced Parkinson's disease," *Journal of Neurology, Neurosurgery & Psychiatry*, vol. 62, pp. 133-140, 1997.

[6] T. S. Staff, T. S. Ahearn, K. Wilson, C. E. Counsell, K. Taylor, R. Caslake, J. E. Davidson, H. G. Gemmell, and A. D. Murray, "Shape analysis of 123I-N-ω-fluoropropyl-2-β-carbomethoxy-3β-(4-iodophenyl) nortropane single-photon emission computed tomography images in the assessment of patients with parkinsonian syndromes," *Nuclear Medicine Communications*, vol. 30, pp. 194–201, 2009.

[7] R. Prashanth, S. D. Roy, S. Ghosh, and P. K. Mandal, "Shape features as biomarkers in early Parkinson's disease," in *Neural Engineering (NER), 2013 6th International IEEE/EMBS Conference on*, 2013, pp. 517-520.

[8] D. J. Towey, P. G. Bain, and K. S. Nijran, "Automatic classification of 123I-FP-CIT (DaTSCAN) SPECT images," *Nuclear medicine communications*, vol. 32, pp. 699-707, 2011.

[9] A. Rojas, J. Górriz, J. Ramírez, I. Illán, F. J. Martínez-Murcia, A. Ortiz, M. Gómez Río, and M. Moreno-Caballero, "Application of empirical mode decomposition (EMD) on DaTSCAN SPECT images to explore Parkinson disease," *Expert Systems with Applications*, vol. 40, pp. 2756-2766, 2013.

[10] I. Illan, J. Górriz, J. Ramírez, F. Segovia, J. Jimenez-Hoyuela, and S. O. Lozano, "Automatic assistance to Parkinson's disease diagnosis in DaTSCAN SPECT imaging," *Medical physics*, vol. 39, pp. 5971-5980, 2012.

[11] F. Segovia, J. Górriz, J. Ramírez, I. Álvarez, J. Jiménez-Hoyuela, and S. Ortega, "Improved Parkinsonism diagnosis using a partial least squares based approach," *Medical physics*, vol. 39, pp. 4395-4403, 2012.

[12] C. Scherfler and M. Nocker, "Dopamine transporter SPECT: How to remove subjectivity?," *Movement Disorders*, vol. 24, pp. S721-S724, 2009.

[13] J. Seibyl, D. Jennings, C. Coffey, and K. Marek, "Multicenter evaluation of Parkinson's disease progression using 123-I I-Ioflupane SPECT: Update from the Parkinson's progression marker initiative trial," in *Movement Disorders*, 2014, pp. S94-S94.

[14] J. Seibyl, D. Jennings, I. Grachev, C. Coffey, and K. Marek, "123-I Ioflupane SPECT Measures of Parkinson Disease Progression in the Parkinson Progression Marker Initiative (PPMI) Trial," in *Society of Nuclear Medicine Annual Meeting Abstracts*, 2013, p. 190.

[15] L. G. Apostolova, M. Beyer, A. E. Green, K. S. Hwang, J. H. Morra, Y. Y. Chou, C. Avedissian, D. Aarsland, C. C. Janvin, and J. P. Larsen, "Hippocampal, caudate, and ventricular changes in Parkinson's disease with and without dementia," *Movement Disorders*, vol. 25, pp. 687-695, 2010.

[16] N. Faggian, Z. Chen, L. Johnston, O. Se-Hong, Z.-H. Cho, and G. Egan, "A method for Shape Analysis and Segmentation in MRI," in *Digital Image Computing: Techniques and Applications (DICTA), 2008*, 2008, pp. 335-342.

[17] V. Sossi, R. de la Fuente-Fernández, J. E. Holden, M. Schulzer, T. J. Ruth, and J. Stoessl, "Changes of Dopamine Turnover in the Progression of Parkinson's Disease as Measured by Positron Emission Tomography: Their Relation to Disease-Compensatory Mechanisms," *Journal of Cerebral Blood Flow & Metabolism*, vol. 24, pp. 869-876, 2004.

[18] N. Ilgin, J. Zubieta, S. Reich, R. Dannals, H. Ravert, and J. Frost, "PET imaging of the dopamine transporter in progressive supranuclear palsy and Parkinson's disease," *Neurology*, vol. 52, pp. 1221-1221, 1999.

[19] E. Nurmi, H. M. Ruottinen, J. Bergman, M. Haaparanta, O. Solin, P. Sonninen, and J. O. Rinne, "Rate of progression in Parkinson's disease: A 6-[18F] fluoro-L-dopa PET study," *Movement Disorders*, vol. 16, pp. 608-615, 2001.